Am J Physiol Heart Circ Physiol 283: H193–H203, 2002;
10.1152/ajpheart.00026.2001.

CaMKII-dependent reactivation of SR Ca^{2+} uptake and contractile recovery during intracellular acidosis

NORIYUKI NOMURA,[1] HIROSHI SATOH,[1] HAJIME TERADA,[1] MASAKI MATSUNAGA,[1]
HIROSHI WATANABE,[2] AND HIDEHARU HAYASHI[1]
[1]*Division of Cardiology, Internal Medicine III, and* [2]*Clinical Pharmacology and Therapeutics, Hamamatsu University School of Medicine, Hamamatsu 431-3192, Japan*

Received 18 January 2001; accepted in final form 21 March 2002

Nomura, Noriyuki, Hiroshi Satoh, Hajime Terada, Masaki Matsunaga, Hiroshi Watanabe, and Hideharu Hayashi. CaMKII-dependent reactivation of SR Ca^{2+} uptake and contractile recovery during intracellular acidosis. *Am J Physiol Heart Circ Physiol* 283: H193–H203, 2002; 10.1152/ajpheart.00026.2001.—In hearts, intracellular acidosis disturbs contractile performance by decreasing myofibrillar Ca^{2+} response, but contraction recovers at prolonged acidosis. We examined the mechanism and physiological implication of the contractile recovery during acidosis in rat ventricular myocytes. During the initial 4 min of acidosis, the twitch cell shortening decreased from 2.3 ± 0.3% of diastolic length to 0.2 ± 0.1% (means ± SE, $P < 0.05$, $n = 14$), but in nine of these cells, contractile function spontaneously recovered to 1.5 ± 0.3% at 10 min ($P < 0.05$ vs. that at 4 min). During the depression phase, both the diastolic intracellular Ca^{2+} concentration ($[Ca^{2+}]_i$) and Ca^{2+} transient (CaT) amplitude increased, and the twitch $[Ca^{2+}]_i$ decline prolonged significantly ($P < 0.05$). In the cells that recovered, a further increase in CaT amplitude and a reacceleration of twitch $[Ca^{2+}]_i$ decline were observed. The increase in diastolic $[Ca^{2+}]_i$ was less extensive than the increase in the cells that did not recover ($n = 5$). Blockade of sarcoplasmic reticulum (SR) function by ryanodine (10 μM) and thapsigargin (1 μM) or a selective inhibitor of Ca^{2+}-calmodulin kinase II, 2-[*N*-(2-hydroxyethyl)-*N*-(4-methoxybenzenesulfonyl)] amino-*N*-(4-chlorocinnamyl)-*N*-methyl benzylamine (1 μM) completely abolished the reacceleration of twitch $[Ca^{2+}]_i$ decline and almost eliminated the contractile recovery. We concluded that during prolonged acidosis, Ca^{2+}-calmodulin kinase II-dependent reactivation of SR Ca^{2+} uptake could increase SR Ca^{2+} content and CaT amplitude. This recovery can compensate for the decreased myofibrillar Ca^{2+} response, but may also cause Ca^{2+} overload after returning to physiological pH_i.

cardiac myocyte; intracellular pH; intracellular Ca^{2+} concentration; ATPase

THE CONTROL OF INTRACELLULAR pH (pH_i) is important in virtually all tissues, and intracellular acidosis has profound effects on various cellular functions. In hearts, intracellular acidosis as a major component of myocardial ischemia or as a result of renal or respiratory failure disturbs the electrical and mechanical performances. In ischemic hearts, reperfusion is necessary for the functional recovery, but it is not always beneficial to the damaged myocardium and causes an additional myocardial injury. A phenomenon in which rapid return from acidotic to physiological pH_i produces undesirable secondary effects (termed the "pH paradox") has been recognized to be a factor for reperfusion cell injury (8, 21).

Intracellular acidosis exerts substantial effects on contractile performance and intracellular Ca^{2+} metabolism in cardiac myocytes. These include a decrease in twitch contraction, a prolongation of relaxation, an increase in the Ca^{2+} transient (CaT) amplitude, and a decrease in the rate of twitch intracellular Ca^{2+} concentration ($[Ca^{2+}]_i$) decline (5, 15, 19, 35). Previous studies (12, 34) have indicated that the decrease in twitch contraction is caused principally by a decreased Ca^{2+} responsiveness of contractile proteins.

Although twitch contraction rapidly decreases in the initial minutes of acidosis, it slowly recovers (15, 19, 24, 35). The mechanism of the contractile recovery remains undefined, but the increase in CaT amplitude, which overcomes the decreased Ca^{2+} responsiveness of contractile proteins, has been suggested (15, 19). The increase in $[Ca^{2+}]_i$ during acidosis seems to be due to two mechanisms: displacement of Ca^{2+} from intracellular buffering sites (24, 35) and activation of Na^+/H^+ exchange by an increase in intracellular $[H^+]$ (15). The activation of Na^+/H^+ exchange increases $[Na^+]_i$ which, in turn, increases $[Ca^{2+}]_i$ via Na^+/Ca^{2+} exchange (36).

In mammalian hearts, the sarcoplasmic reticulum (SR) plays a dominant role both in the contraction and relaxation processes (5). Previous in vitro studies have shown that acidosis directly inhibits the SR Ca^{2+}-ATPase (12) and the SR Ca^{2+} release channels (ryanodine receptors) (1, 44). Moreover, acidosis decreases (or does not change) the Ca^{2+} entry via the L-type Ca^{2+} channels (11, 19, 20). These inhibitory effects are expected to reduce the total SR Ca^{2+} content, suppress the Ca^{2+}-induced Ca^{2+} release (CICR) from the SR, and decrease the CaT amplitude (3).

Address for reprint requests and other correspondence: H. Satoh, Div. of Cardiology, Internal Medicine III, Hamamatsu University School of Medicine, 1-20-1 Handayama, Hamamatsu 431-3192, Japan (E-mail: satoh36@hama-med.ac.jp).

The costs of publication of this article were defrayed in part by the payment of page charges. The article must therefore be hereby marked "*advertisement*" in accordance with 18 U.S.C. Section 1734 solely to indicate this fact.

Here we hypothesized that the reactivation of SR Ca^{2+}-ATPase might be another mechanism for the increase in CaT amplitude during prolonged acidosis. The SR Ca^{2+}-ATPase is activated through phosphorylation of phospholamban (PLB) and also by its direct phosphorylation (5, 28, 38, 40). Because $[Ca^{2+}]_i$ increases during intracellular acidosis, the Ca^{2+}-calmodulin-dependent kinase II (CaMKII) is a possible candidate for the reactivation of SR Ca^{2+}-ATPase. CaMKII is highly enriched in the nervous system and mediates many actions of Ca^{2+} (37). In cardiac myocytes, CaMKII phosphorylates several proteins and modulates the excitation-contraction coupling (4, 14, 27, 43, 45).

In this study, we examined the effects of two types (respiratory and metabolic) of prolonged acidosis on the twitch contraction and CaT in isolated rat myocytes, and tried to clarify the mechanism and physiological implication of the recovery of twitch contraction. Our results indicate that the reactivation of SR Ca^{2+} uptake caused by CaMKII activation during prolonged acidosis can reaccelerate the twitch $[Ca^{2+}]_i$ decline, increase the SR Ca^{2+} content and the CaT amplitude, and thereafter induce the contractile recovery.

MATERIALS AND METHODS

Isolation of ventricular myocytes. This investigation conforms with the *Guide for the Care and Use of Laboratory Animals* published by the National Institutes of Health. Ventricular myocytes were isolated from male Sprague-Dawley rats (220–300 g) and were stocked in the modified Kraftbrühe (KB) solution as described previously (16). Composition of the modified KB solution was as follows (in mM): 70 KOH, 40 KCl, 20 KH_2PO_4, 3 $MgCl_2$, 50 glutamic acid, 10 glucose, 10 HEPES, and 0.5 EGTA (pH 7.4 with KOH). Before the start of experiments, the modified KB solution was replaced with a Krebs solution containing (in mM) 113.1 NaCl, 4.6 KCl, 1.2 $MgCl_2$, 3.5 NaH_2PO_4, 21.9 $NaHCO_3$, 1.5 $CaCl_2$, and 10 glucose, or a HEPES-buffered solution that contained (in mM) 137 NaCl, 4 KCl, 1.2 $MgSO_4$, 10 glucose, 10 HEPES, and 1.5 $CaCl_2$, with pH adjusted to 7.4 with NaOH.

Loading of fluorescent indicators. Myocytes were loaded with indo-1-acetoxymethyl ester (indo-1-AM; 10 μM) for 10 min at room temperature. The stock solution of indo-1-AM was prepared by mixing 1 mg of dye in dry dimethyl sulfoxide and was kept frozen in aliquots until use. Immediately before use, the dyes were dissolved with KB solution containing 1% bovine serum albumin and 0.075% Pluronic F-127 (wt/vol, final concentration). The myocytes were then washed twice in a modified KB solution and were incubated for 30 min to complete hydrolysis of dyes. For the measurement of pH_i, the cells were loaded with 2′,7′-bis (carboxyethyl)-5,6-carboxyfluorescein (BCECF)-AM (1 μM) for 30 min at room temperature and were then washed and incubated as mentioned above.

Apparatus. After fluorescent indicators were loaded, a small aliquot of myocytes were placed in an experimental chamber mounted on the stage of an inverted microscope (TMD, Nikon; Tokyo, Japan), and perfused with Krebs or HEPES solution at room temperature. The myocytes were field stimulated through platinum electrodes at 0.5 Hz, and were illuminated by a transmitted illuminator or ultraviolet light via an epifluorescence illuminator from a 100-W xenon lamp equipped with an interference filter.

For the simultaneous measurement of $[Ca^{2+}]_i$ and cell length in single myocytes, we designed an optical system with an inverted microscope (23). To measure $[Ca^{2+}]_i$, indo-1-loaded myocytes were excited at 340 nm, and the emission signal was separated into 405- and 485-nm wavelengths with the appropriate dichroic mirror and band-pass filters. Both fluorescent signals were sampled by two photomultipliers (model R1332, Hamamatsu Photonics; Hamamatsu, Japan) with a photon-counting unit (model C3866, Hamamatsu Photonics). The fluorescent ratios were obtained by dividing the fluorescent intensity at 405 nm by the fluorescent intensity at 480 nm after each background subtraction. The cells were simultaneously illuminated with red light (>600 nm) through the normal bright-field illumination optics. The bright-field image was separated from the fluorescence image by a 580-nm long-pass dichroic mirror. The cell image was focused on the linear image sensor (model S3904–2048Q, Hamamatsu Photonics) that consisted of 2,048 photodiodes. Light intensity of each photodiode was scanned at a rate of 1.5 μs per photodiode and monitored on the oscilloscope continuously. Both edges of a cell were identified by the edge-detection system (model MOS-SPL 46A001, Hamamatsu Photonics) and cell lengths were computed from the numbers of photodiodes between each edge. Signals from the photomultipliers and the edge-detection system were monitored and stored in a microcomputer (PC-9801 DA, NEC; Tokyo, Japan) at the sampling frequency of 200 Hz via a 12-bit analog-to-digital converter, and off-line analysis was conducted.

In the measurement of pH_i, the fluorescent signal was imaged with a silicon-intensified target camera (model C2400, Hamamatsu Photonics), with the output digitized to a resolution of 512 × 512 pixels by an image analysis system (Argus 50, Hamamatsu Photonics). The exciting wavelengths were 490 and 450 nm and an emission wavelength was at 505–560 nm. Each image was the accumulation of eight (30 s) successive video frames and the fluorescence intensity was obtained by dividing, pixel by pixel, the 490 × 450-nm image after each background subtraction. To minimize photobleaching, exposure to excitation light was limited during data collection (0.27 s per collection) by an electrically controlled shutter, and neutral density filters were placed in the exciting light paths.

Calibration of BCECF fluorescence. We conducted an in vivo calibration in the preliminary cell group, according to the method previously described (16). BCECF-loaded myocytes were perfused with the calibration solutions, which contained 10 μM nigericin in the following solution (in mM): 130 KCl, 15 MgCl2, 1 2-(*N*-morpholino)ethanesulfonic acid, and 15 HEPES. The pH was adjusted appropriately with KOH. Fluorescence ratios were linearly related to pH_i from 6.5 to 7.5.

Experimental protocol. The myocytes that showed potentiation of twitch after 30 s of rest (postrest potentiation) were selected, and those in which the diastolic $[Ca^{2+}]_i$ exceeded 200 nM or the spontaneous contractions during rest occurred were excluded from the analyses. In the present study, two types of acidosis were applied. For respiratory acidosis, increasing the percentage of CO_2 equilibrated with the bicarbonate buffer from 5 to 30% reduced pH_i by 0.32 pH units (Fig. 1*A*, $n = 10$). The time constant of pH_i change was ~1.0 min, and stable acidosis was achieved up to 15 min. On returning to the control perfusate gassed with 5% CO_2, pH_i recovered to its control value without exhibiting an overshoot. For metabolic acidosis, the myocytes were superfused

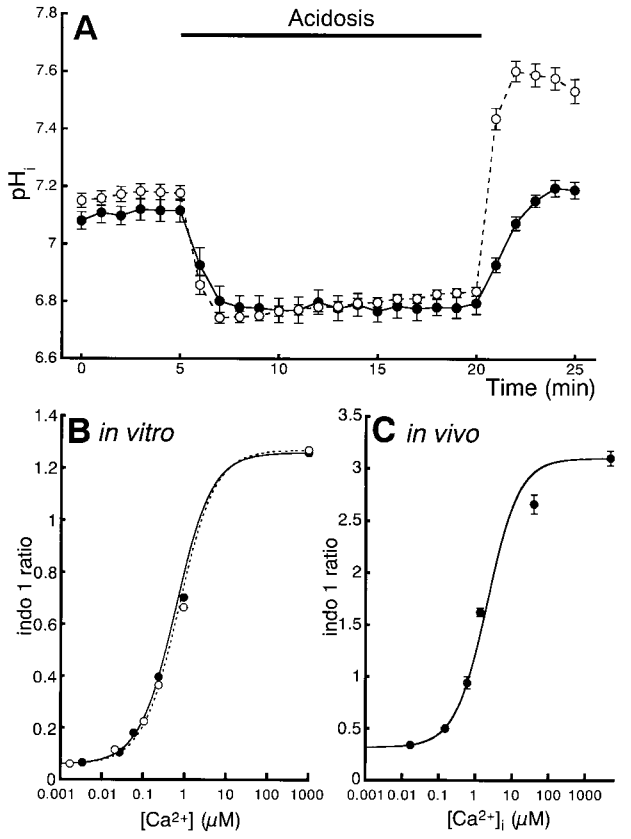

Fig. 1. Changes in intracellular pH (pH_i) during respiratory and metabolic acidosis and the effect of pH_i on indo-1 calibration curves. *A*: rapid and stable intracellular acidosis (ΔpH: ~0.35) was obtained by increasing the percentage of CO_2 in the bicarbonate buffer from 5 to 30% (respiratory acidosis; ● on solid trace), or by adding sodium propionate (20 mM) in HEPES solution at pH 6.8 (metabolic acidosis; ○ on dashed trace). On returning to the control perfusate, pH_i rapidly recovered to the control values and at metabolic acidosis, a transient alkaline overshoot was observed. Values are means ± SE from 10 experiments (2 rats). *B*: in vitro calibration curves of indo-1 fluorescence at pH 7.2 (solid line and ●) and at pH 6.8 (dotted line and ○). Free Ca^{2+} concentrations ($[Ca^{2+}]$) in calibration solutions were corrected with the use of proper dissociation constants (K_d) of EGTA for Ca^{2+} (151 nM at pH 7.2 and 940 nM at pH 6.8). The fluorescence ratios at different levels of $[Ca^{2+}]$ were plotted and were fitted using the formula $[Ca^{2+}] = K_d \times (S_f/S_b) \times (R - R_{min})/(R_{max} - R)$, where R_{min} and R_{max} are the ratios at zero and saturating $[Ca^{2+}]$, S_f/S_b is the ratio of fluorescence at 485 nm at zero and saturating $[Ca^{2+}]$. The obtained values of R_{max} and R_{min} were almost identical between pH 7.2 and 6.8, but the K_d at pH 6.8 was 1.2-fold larger (see MATERIALS AND METHODS). *C*: in vivo calibration curve of indo-1 fluorescence at pH 7.2. The K_d at pH 7.2 was 786 nM, S_f/S_b was 3.3, R_{max} and R_{min} were 3.1 and 0.31, respectively. Under the acidic perfusion, the K_d was assumed to be 943 nM. $[Ca^{2+}]_i$, intracellular $[Ca^{2+}]$. Values are means ± SE from 20 experiments (2 rats).

with HEPES solution containing sodium propionate (20 mM) with pH 6.8. The pH_i decreased by 0.38 pH units and a stable acidosis was obtained as respiratory acidosis, but on returning to the control HEPES solution, pH_i exhibited an alkaline overshoot (Fig. 1*A*, $n = 10$).

Calibration of indo-1 fluorescence. A major problem for $[Ca^{2+}]_i$ measurement in our experiments is the direct effect of pH_i on indo-1 fluorescence (25). We first compared in vitro calibration curves of indo-1 fluorescence between pH 7.2 and 6.8. Because the free $[Ca^{2+}]$ in calibration solutions (calcium calibration buffer kits; Molecular Probes) are also affected by the change in pH, we corrected them with the use of proper dissociation constants (K_d) of EGTA for Ca^{2+} (151 nM at pH 7.2 and 940 nM at pH 6.8). Thus the calibration curves were made with two series of different $[Ca^{2+}]$ (3.4, 27, 60, 237, and 951 nM and 1 mM at pH 7.2 and 1.7, 21, 106, 238, and 937 nM and 1 mM at pH 6.8) (Fig. 1*B*). The indo-1 fluorescence ratios at different levels of $[Ca^{2+}]$ were fitted using the formula $[Ca^{2+}] = K_d \times (S_f/S_b) \times (R - R_{min})/(R_{max} - R)$, where R_{min} and R_{max} are the ratios at zero and saturating $[Ca^{2+}]$, (S_f/S_b) is the ratio of fluorescence at 485 nm at zero and saturating $[Ca^{2+}]$ (13). The obtained values of R_{max} and R_{min} were almost identical between pH 7.2 and 6.8 (R_{max}, 1.26 and 1.27, and R_{min}, 0.06 and 0.06), but the K_d at pH 6.8 was 1.2-fold larger (375 and 419 nM). Subsequently, we performed in vivo calibration, in the preliminary cell group using calibration solutions with different $[Ca^{2+}]_i$ (17, 150, and 600 nM, 1.35, 39.6 μM and 5 mM) at pH_i 7.2. The K_d was 786 nM, (S_f/S_b) was 3.3, and R_{max} and R_{min} were 3.10 and 0.31, respectively (Fig. 1*C*). Under the control perfusion with pH 7.4, we applied these values for calculation of $[Ca^{2+}]_i$, and under acidic perfusion, the K_d was assumed to be 943 nM (786 nM × 1.2; from in vitro calibration).

Reagents and solutions. BCECF-AM and indo-1-AM were supplied from Molecular Probes. Thapsigargin, ryanodine, and cantharidin were purchased from Sigma. BAY K 8644 was obtained from Calbiochem. 2-[*N*-(2-hydroxyethyl)-*N*-(4-methoxybenzenesulfonyl)] amino-*N*-(4-chlorocinnamyl)-*N*-methyl benzylamine (KN-93) was purchased from Seikagaku and isoproterenol was purchased from Wako. These reagents were used from stock solutions in water or dimethyl sulfoxide, and were added to the perfusate immediately before use. The final concentration of dimethyl sulfoxide was not >0.1%, and each reagent produced neither change in cellular autofluorescence nor fluorescence artifact by itself.

Statistical analysis. Results were expressed as means ± SE for the indicated number (n) of myocytes. The number of animals that generated cell samples was also shown. Because several myocytes were derived from the same rat, it was verified by a nested ANOVA procedure that the heterogeneity of cellular responses was dependent on the individual myocytes rather than differences among rats. Changes in parameters of cell shortening and CaT were then estimated by repeated-measures ANOVA for overall effects of the treatments. The differences in each parameter within treatments were compared with the use of ANOVA, followed by Bonferroni's modified t-test. The proportions of recovered cells among treatments were compared using Fisher's exact probability test. The comparisons of baseline cell shortening and CaT between the cells that recovered and did not recover were performed with the use of an unpaired Student's t-test. The probability was considered significant at $P < 0.05$.

RESULTS

Effects of respiratory acidosis on twitch cell contraction and CaT. Figure 2*A* shows a representative example of the changes in steady-state (SS) twitch cell contraction during respiratory acidosis. The simultaneous records of CaT in Fig. 2*B* were obtained at the times indicated by the letters in Fig. 2*A* at 10 min of control perfusion, 4 min and 10 min during respiratory acidosis, and 2 min after reperfusion with control Krebs solution, respectively. Respiratory acidosis quickly decreased the twitch contraction but slightly increased both the diastolic $[Ca^{2+}]_i$ and CaT amplitude. Contraction reached a nadir at ~4 min, but

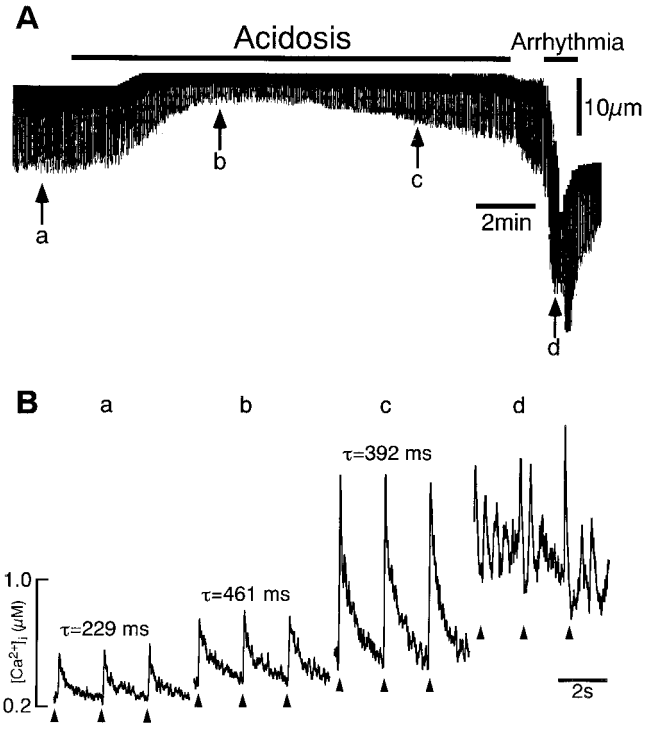

Fig. 2. Effects of respiratory acidosis on twitch cell shortening and Ca^{2+} transient (CaT) in a rat ventricular myocytes loaded with indo-1. *A*: continuous record of twitch cell shortening (0.5 Hz) from a typical experiment. Respiratory acidosis as indicated by bar was obtained by increasing the percentage of CO_2 in bicarbonate buffer from 5 to 30%. *B*: CaT obtained at the times indicated by the lowercase letters in *A* at control perfusion (*a*), 4 min (*b*), and 10 min (*c*) during respiratory acidosis and 2 min after reperfusion (*d*) with control solution, respectively. Each time constant (τ) of twitch $[Ca^{2+}]_i$ decline is also shown. Arrowheads indicate electrical stimuli at 0.5 Hz.

thereafter slowly recovered. The recovery was accompanied by larger increases in both the diastolic $[Ca^{2+}]_i$ and CaT amplitude. After washout of the acidic solution, both the twitch contraction and $[Ca^{2+}]_i$ increased, but then spontaneous contractions and $[Ca^{2+}]_i$ oscillation occurred within 5 min, indicating cellular Ca^{2+} overload. The averaged changes of twitch contraction and CaT were analyzed in 14 myocytes (8 rats, Table 1). We defined the time at minimum contraction as depression phase (DP; 4.2 ± 0.3 min). Because the contractile recovery was visually apparent when contraction exceeded 1% of diastolic length, this value was chosen to determine whether the recovery occurred or not. The contractile recovery was generally prominent by 10 min, and we took this time point (10 min) as the recovery phase (RP). Both the diastolic $[Ca^{2+}]_i$ and CaT amplitude increased significantly at DP and increased further at RP, whereas the diastolic cell length or time to peak of CaT did not change. The SR Ca^{2+} contents were also examined by discharging SR Ca^{2+} with a rapid application of caffeine (10 mM) (2). In this experiment, the perfusate $[Ca^{2+}]$ was reduced to 0.8 mM to prevent Ca^{2+} overload. The amplitude of caffeine-induced CaT increased significantly at DP and increased further at RP (Table 1).

Cell-to-cell heterogeneity in recovery of twitch contraction during respiratory acidosis. In our experimental protocol, the initial decrease in twitch contraction occurred in all myocytes, but the contractile recovery was evident in 9 of 14 cells (64%: 1.5 ± 0.3% of diastolic length at RP; $P < 0.05$ vs. that at DP). To investigate the underlying mechanism for this cell-to-cell heterogeneity, we compared possible parameters of twitch contraction and CaT between the cells that recovered (Rec: $n = 9$) and did not recover (NRec: $n = 5$). There was no significant difference in twitch contraction (2.4 ± 0.4% and 2.2 ± 0.6% of diastolic length), diastolic $[Ca^{2+}]_i$ (132 ± 15 and 141 ± 15 nM), or CaT amplitude (378 ± 66 and 323 ± 45 nM) at control perfusion. In Rec, the CaT amplitude continuously increased (Fig. 3*A*), whereas in NRec, the CaT amplitude did not increase (from 389 ± 60 nM at DP to 240 ± 67 nM at RP, P = not significant). On the other hand, the increase in diastolic $[Ca^{2+}]_i$ from DP to RP was more evident in NRec (300 ± 54 to 387 ± 69 nM, $P < 0.05$).

These findings indicate that respiratory acidosis initially depresses the twitch cell contraction by decreasing the response of myofilaments to Ca^{2+}, but the contraction recovers subsequently by the increase in CaT amplitude (presumably due to increased SR Ca^{2+} content).

Effects of respiratory acidosis on rate of twitch $[Ca^{2+}]_i$ decline. The SR Ca^{2+} content is determined both by $[Ca^{2+}]_i$ and by Ca^{2+} uptake through the SR

Table 1. *Effects of respiratory acidosis on SS twitches and SR Ca^{2+} load*

	n	CTL	DP	RP
Diastolic cell length, μm	14(8)	117.2 ± 4.4	117.6 ± 4.4	117.5 ± 4.4
SS contraction at 0.5 Hz, μm	14(8)	2.7 ± 0.3	0.3 ± 0.1*	1.2 ± 0.3*
SS contraction, %	14(8)	2.3 ± 0.3	0.2 ± 0.1*	1.0 ± 0.2*
Diastolic $[Ca^{2+}]_i$, nM	14(8)	135 ± 10	242 ± 25*	301 ± 32*†
SS twitch CaT amplitude, nM	14(8)	358 ± 43	448 ± 52*	539 ± 104*†
Time to peak Ca^{2+} transient, ms	14(8)	61 ± 1	66 ± 2	66 ± 2
Caffeine-induced CaT amplitude, nM	5(4)	520 ± 215	738 ± 224*	834 ± 276*†

Values are means ± SE; n = no. of myocytes. The number of animals that generate cell samples are shown in parentheses. CaT, Ca transient amplitude, i.e., increase in intracellular Ca^{2+} concentration ($[Ca^{2+}]_i$) above diastolic $[Ca^{2+}]_i$ during steady-state (SS) twitch or caffeine application; %, percentage of resting cell length; CTL, control; DP, depression phase; RP, recovery phase. In measurement of caffeine-induced CaT amplitude, perfusate $[Ca^{2+}]$ was reduced to 0.8 mM to prevent Ca^{2+} overload. *$P < 0.05$ vs. CTL, †$P < 0.05$ vs. DP by ANOVA, followed by Bonferroni's-modified *t*-test.

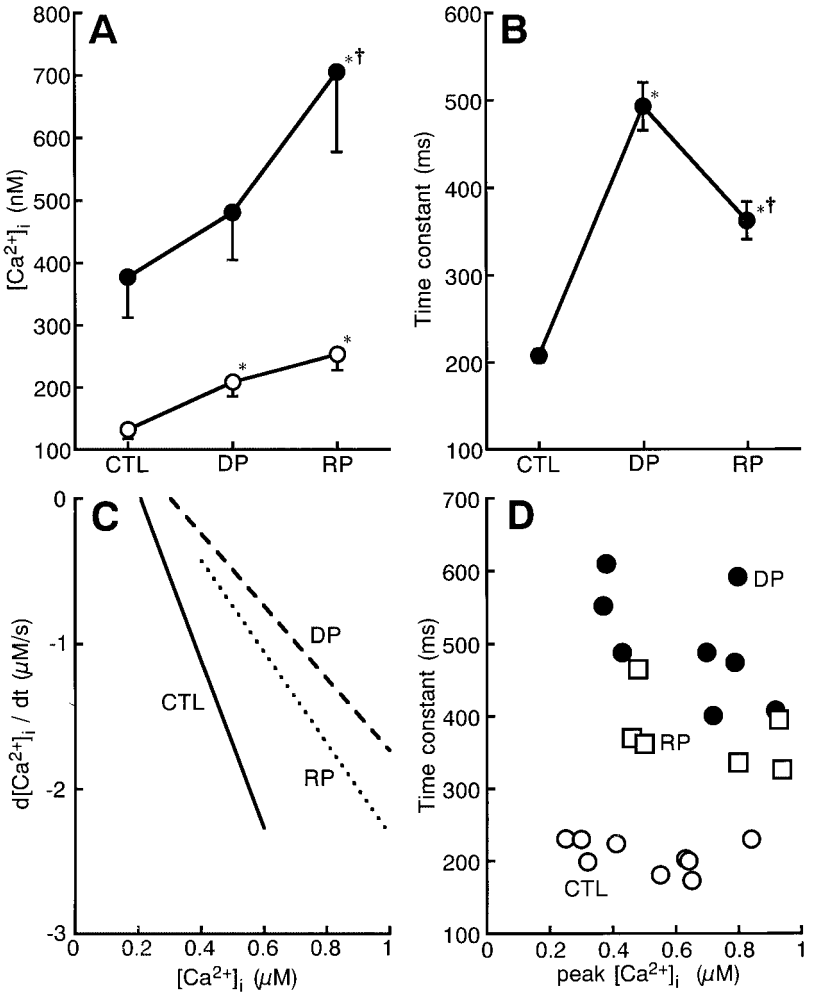

Fig. 3. Acidosis induced changes in the profile of CaT in the cells that twitch contraction recovered (Rec). *A*: steady-state CaT amplitude (●) and diastolic $[Ca^{2+}]_i$ (○) during control perfusion (CTL), at depression phase (DP), and recovery phase (RP) during respiratory acidosis. *B*: time constants of twitch $[Ca^{2+}]_i$ decline obtained from single exponential fits. Values are means ± SE from 9 myocytes (6 rats). $*P < 0.05$ vs. the values at CTL, $\dagger P < 0.05$ vs. those at DP by analysis of variance (ANOVA), followed by Bonferroni-modified *t*-test. *C*: plots of rates of $[Ca^{2+}]_i$ decline ($d[Ca^{2+}]_i/dt$) against $[Ca^{2+}]_i$ at CTL (solid line), DP (dashed line), and RP (dotted line) in a representative example. *D*: time constants of twitch $[Ca^{2+}]_i$ decline against their peak $[Ca^{2+}]_i$ at CTL (○), DP (●), and RP (□). In (*C*) and (*D*), the $[Ca^{2+}]_i$ values in the *x*-axis was limited <1 μM to make the difference between DP and RP more apparent. The plotted number of DP and RP therefore decreased to eight and six, respectively.

Ca^{2+}-ATPase (5). Because the increase in CaT amplitude during acidosis was accompanied by the increase in the SR Ca^{2+} content but was not simply dependent on diastolic $[Ca^{2+}]_i$, the increase in the SR Ca^{2+} content may be due to reactivation of SR Ca^{2+} uptake. In mammalian ventricular myocytes, the SR Ca^{2+} uptake can be estimated from the rate of twitch $[Ca^{2+}]_i$ decline (6, 19). Figure 3*B* shows the mean time constants (τ) of twitch $[Ca^{2+}]_i$ decline obtained from single exponential fits. The $[Ca^{2+}]_i$ decline slowed in all cells at DP but reaccelerated at RP in Rec (see also Fig. 2*B*). In NRec, such a reacceleration was never seen. However, the rate of twitch $[Ca^{2+}]_i$ decline depends on the range of $[Ca^{2+}]_i$ over which it is measured (6). Because the CaT amplitude increased during acidosis, the observed change in the time constant might reflect the change in amplitude rather than that in SR Ca^{2+} uptake. To rule out this possibility, the rate of twitch $[Ca^{2+}]_i$ decline in a given $[Ca^{2+}]_i$ was investigated. The exponential curve fitted to the declining phase of CaT was differentiated to give the rate of change of $[Ca^{2+}]_i$ ($d[Ca^{2+}]_i/dt$) and plotted against $[Ca^{2+}]_i$ (Fig. 3*C*, see also Ref. 19). The $d[Ca^{2+}]_i/dt$ decreased in any given $[Ca^{2+}]_i$ at DP, but partially recovered at RP. Similar results were obtained in all of Rec. Figure 3*D* also indicates that the time constants of twitch $[Ca^{2+}]_i$ decline recovered at RP for similar peak $[Ca^{2+}]_i$. Thus the reacceleration of $[Ca^{2+}]_i$ decline at RP was not secondary to the increase in CaT amplitude.

Effects of metabolic acidosis on twitch cell contraction and CaT. Metabolic acidosis (with 20 mM propionate, pH 6.8) produced changes similar to those in respiratory acidosis. Seven of fourteen myocytes (10 rats) showed contractile recovery, whereas the remaining seven cells did not. In Rec, the CaT amplitude increased from 320 ± 73 nM at control to 464 ± 64 nM at DP and to 656 ± 129 nM at RP, whereas the increase in diastolic $[Ca^{2+}]_i$ was small (from 417 ± 76 nM at DP to 429 ± 101 nM at RP). The twitch $[Ca^{2+}]_i$ decline initially slowed in all of the cells but reaccelerated in Rec (τ: 442 ± 26 ms at DP and 310 ± 15 ms at RP, $P < 0.05$). In NRec, neither the large increase in CaT amplitude nor the reacceleration of the twitch $[Ca^{2+}]_i$ decline was observed, while the diastolic $[Ca^{2+}]_i$ continued to increase (data not shown). However, soon after returning to control HEPES solution, all the cells exhibited hypercontracture. This morphological change was possibly ascribed to both Ca^{2+} overload and augmented myo-

fibrillar Ca^{2+} responsiveness by an alkaline overshoot.

Inhibition of the SR function and acidosis-induced changes in twitch cell contraction and CaT. To investigate further the correlation between the contractile recovery and the SR Ca^{2+} uptake, the twitch cell contraction and CaT were monitored in the cells where the SR function was abolished with thapsigargin (1 μM) and ryanodine (10 μM). For this experiment, Ca^{2+} influx via sarcolemmal Ca^{2+} channels was increased with BAY K 8644 (100 nM) to make twitch contractions and CaT comparable. BAY K 8644 acts directly to sarcolemmal L-type Ca^{2+} channels and enhances Ca^{2+} currents by increasing open time of the channels (17). The cells were preincubated for 30 min with these agents, and the decreases in twitch contraction and CaT amplitude were limited to ~50%. Figure 4 shows a typical example of myocytes that were electrically stimulated at 0.1 Hz while being perfused with control and acidic solution. The SR inhibition apparently slowed the twitch $[Ca^{2+}]_i$ decline and relaxation. The twitch contraction disappeared soon after the perfusion of acidic solution and never recovered. The diastolic $[Ca^{2+}]_i$ continued to increase, but the increase in CaT amplitude was small. The slow twitch $[Ca^{2+}]_i$ decline prolonged further during acidosis, and reacceleration did not occur. Figure 5 summarizes the changes in twitch contraction (Fig. 5*A*), diastolic $[Ca^{2+}]_i$ and CaT amplitude (Fig. 5*B*), and time constant of twitch $[Ca^{2+}]_i$ decline (Fig. 5*C*) during respiratory acidosis (n = 9, 3 rats). The twitch contraction decreased during acidosis and never recovered in all cells. The diastolic $[Ca^{2+}]_i$ continued to increase, and the CaT amplitude initially increased but soon reached plateau. Respiratory acidosis further slowed the $[Ca^{2+}]_i$ decline, but the reacceleration was never observed. Thus the functional SR was necessary for the reacceleration of twitch $[Ca^{2+}]_i$ decline, increase in CaT amplitude and contractile recovery during prolonged acidosis.

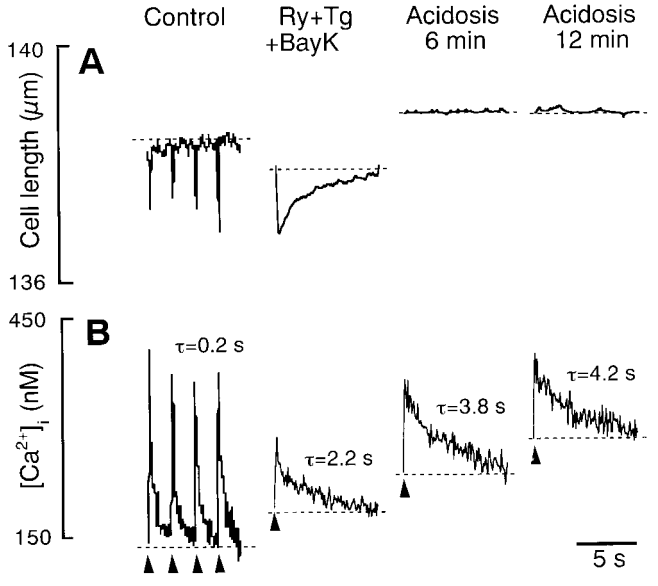

Fig. 4. Effects of respiratory acidosis on twitch cell shortening and CaT in a myocytes in which the SR function was blocked. A representative myocyte preincubated with thapsigargin (Tg; 1 μM) and ryanodine (Ry; 10 μM) for 30 min was exposed to respiratory acidosis. The cell was electrically stimulated at 0.1 Hz and Ca^{2+} influx via L-type Ca^{2+} channels was increased with BAY K 8644 (BayK: 100 nM). The changes in twitch contraction (*A*) and CaT (*B*) during respiratory acidosis were shown. The twitch contraction decreased during acidosis and never recovered. Diastolic $[Ca^{2+}]_i$ continued to increase and the CaT amplitude initially increased but soon reached plateau. SR inhibition largely slowed the twitch $[Ca^{2+}]_i$ decline. The acidosis further slowed the $[Ca^{2+}]_i$ decline but reacceleration was never observed. Dashed lines indicate the baselines of cell shortening and CaT.

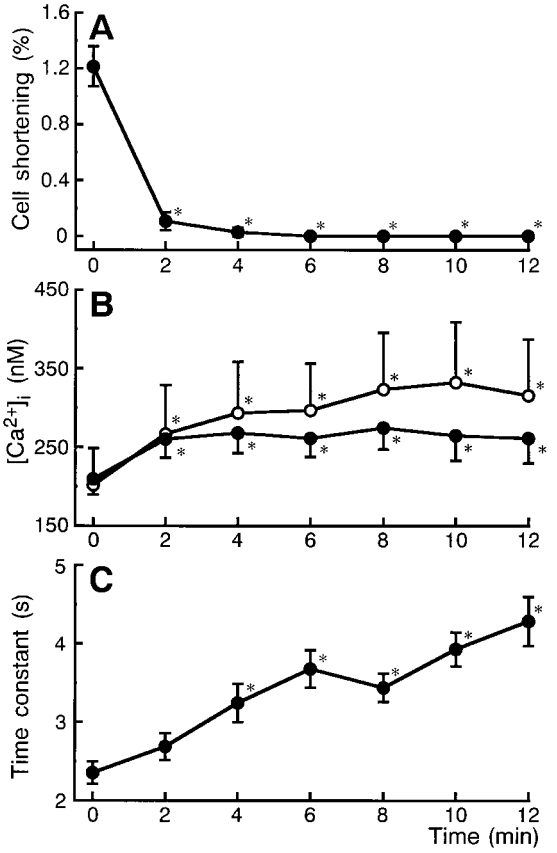

Fig. 5. Effects of SR inhibition on acidosis-induced changes in twitch cell shortening and CaT. Summary data of the changes in twitch contraction (*A*), diastolic $[Ca^{2+}]_i$ (○), and CaT amplitude (●) (*B*), and time constant of twitch $[Ca^{2+}]_i$ decline (*C*) during respiratory acidosis in myocytes where the SR function was blocked. Values are means ± SE from 9 myocytes (3 rats). $^*P < 0.05$ vs. the values at *time 0* by ANOVA, followed by Bonferroni-modified *t*-test.

Acidosis-induced changes in twitch cell contraction and CaT under phosphorylated state. From the experiments above, the reactivation of SR Ca^{2+} uptake was necessary to the reacceleration of twitch $[Ca^{2+}]_i$ decline. The SR Ca^{2+} uptake is activated through phosphorylation of PLB and also through direct phosphorylation of SR Ca^{2+}-ATPase (5, 28, 38, 40). Therefore, the next question is whether the phosphorylation is involved in the reactivation of SR Ca^{2+} uptake during prolonged acidosis. To examine this, the myocytes in normal Krebs solution with 1.5 mM Ca^{2+} were treated with isoproterenol (10 μM) and cantharidin (10 μM),

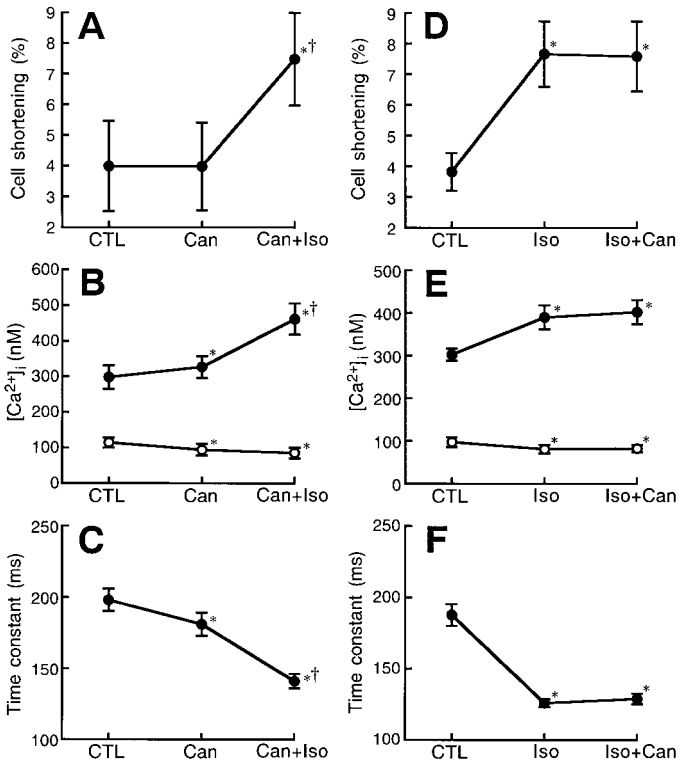

Fig. 6. Effects of isoproterenol (Iso) and cantharidin (Can) on twitch cell shortening and CaT. Changes in twitch contraction (*A* and *D*), diastolic $[Ca^{2+}]_i$ (○) and CaT amplitude (●) (*B* and *E*), and time constant of twitch $[Ca^{2+}]_i$ decline (*C* and *F*). *A–C*: the effects of Can (10 μM) alone and after addition of Iso (10 μM). *D–F*: the effects of Iso alone and after addition of Can were compared. Values are means ± SE from 8 and 9 myocytes (2 and 3 rats, respectively). $*P < 0.05$ vs CTL, $\dagger P < 0.05$ vs. Can by ANOVA, followed by Bonferroni-modified *t*-test.

an inhibitor of protein phosphatases (7) (Fig. 6). Treatment with cantharidin slightly increased the SS CaT amplitude and accelerated the twitch $[Ca^{2+}]_i$ decline but did not change the twitch contraction. The addition of isoproterenol largely augmented these changes and also increased the twitch contraction (Fig. 6, *A–C*). However, application of cantharidin after isoproterenol treatment induced no additive effects on these parameters (Fig. 6, *D–F*). The doses of isoproterenol and cantharidin exhibited maximum effects because higher concentrations of either drug induced no additional changes. Decreasing extracellular $[Ca^{2+}]$ to 0.5 mM matched the SS contraction and CaT amplitude with the preexposed levels but the twitch $[Ca^{2+}]_i$ decline remained accelerated (Fig. 7 and Table 2). Under the condition, contractile recovery during respiratory acidosis never occurred ($n = 12$, 6 rats). The diastolic $[Ca^{2+}]_i$ continued to increase, but CaT amplitude did not change, significantly. The twitch $[Ca^{2+}]_i$ decline prolonged and never recovered.

Effects of KN-93 on acidosis-induced changes in twitch cell contraction and CaT. The PLB and SR Ca^{2+} ATPase are mainly phosphorylated by cAMP-dependent protein kinase (PKA) and CaMKII. Because the increase in CaT amplitude and reacceleration of twitch $[Ca^{2+}]_i$ decline were preceded by the increase in diastolic $[Ca^{2+}]_i$, it was hypothesized that the CaMKII-dependent phosphorylation contributed primarily to the recovery of SR Ca^{2+} uptake. Thus the twitch contraction and CaT were monitored during respiratory acidosis with a selective inhibitor of endogenous CaMKII, KN-93 (1 μM) (39). The perfusion of KN-93 decreased SS twitch contraction, CaT amplitude, and prolonged twitch $[Ca^{2+}]_i$ decline. Increasing extracellular $[Ca^{2+}]$ to 2.5 mM restored SS contraction and CaT amplitude toward the preexposed levels but the twitch $[Ca^{2+}]_i$ decline remained prolonged (Fig. 8 and Table 3). KN-93 did not alter these parameters at the cells in which the SR function was abolished with ryanodine and thapsigargin (data not shown). Contractile recovery during respiratory acidosis was observed in only 3 of 11 cells (27%; from 0.9 ± 0.8% of diastolic length at 4 min to 2.0 ± 0.3% at 10 min, 5 rats). The diastolic $[Ca^{2+}]_i$ continued to increase, but CaT amplitude did not change, significantly. The twitch $[Ca^{2+}]_i$ decline prolonged and never recovered. The effects of KN-93 were also identical at the cells exposed to metabolic acidosis (Table 3). The contractile recovery was seen in only 2 of 11 cells (4 rats).

DISCUSSION

The major findings in the present study are the following: *1*) with prolonged acidosis, there was recov-

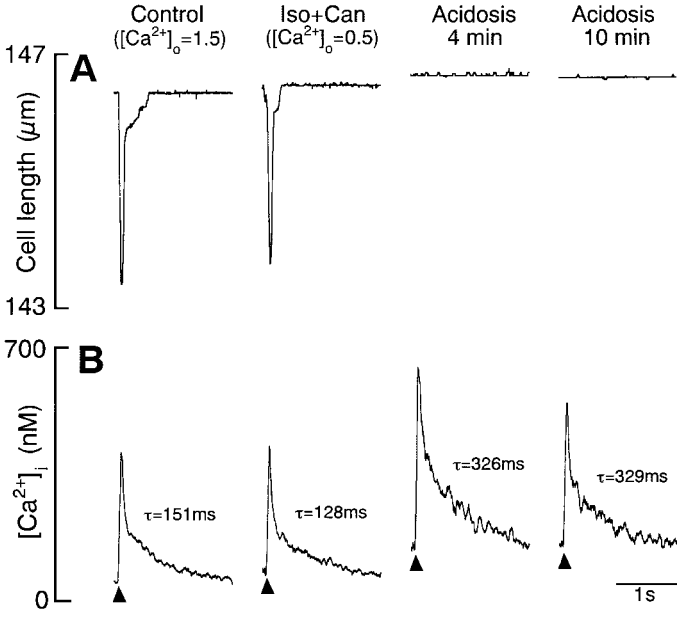

Fig. 7. Effects of phosphorylation on acidosis-induced changes in twitch cell shortening (*A*) and CaT (*B*). Myocytes were initially treated with Iso (10 μM) and Can (10 μM) and then exposed to respiratory acidosis. The pretreatment of a myocyte with Iso and Can increased twitch contraction and CaT amplitude, and shortened the twitch $[Ca^{2+}]_i$ decline. The perfusate $[Ca^{2+}]$ was reduced to 0.5 mM to match the steady-state contraction and CaT amplitude with values at control (Iso + Can). The twitch contraction decreased during acidosis and never recovered. The diastolic $[Ca^{2+}]_i$ continued to increase, and the CaT amplitude did not increase significantly. The acidosis prolonged the $[Ca^{2+}]_i$ decline but reacceleration was never observed. $[Ca^{2+}]_o$, extracellular $[Ca^{2+}]$.

Table 2. *Effects of respiratory acidosis under phosphorylated state*

			Respiratory Acidosis	
	CTL	Iso + Can	4 min (DP)	10 min (RP)
Twitch contraction, %	2.6 ± 0.4	2.2 ± 0.3	0.0 ± 0.0†	0.0 ± 0.0†
Diastolic $[Ca^{2+}]_i$, nM	103 ± 9	75 ± 7	163 ± 15†	186 ± 14†‡
Twitch CaT amplitude, nM	500 ± 55	396 ± 43	533 ± 62†	436 ± 48†
Twitch $[Ca^{2+}]_i$ decline, ms	187 ± 6	139 ± 5*	382 ± 19†	415 ± 19†

Values are means ± SE for 12 myocytes (6 rats). Iso, isoproterenol; Can, cantharidin. In the presence of Iso (10 μM) and Can (10 μM), perfusate $[Ca^{2+}]$ was reduced from 1.5 to 0.5 mM to match the SS twitch contraction and CaT amplitude with values at CTL. *$P < 0.05$ vs. CTL, †$P < 0.05$ vs. Iso + Can, ‡$P < 0.05$ vs. 4 min (DP) by ANOVA, followed by Bonferroni's modified *t*-test.

ery of twitch contractions, which was primarily due to stimulation of SR Ca^{2+} uptake, and *2*) the recovery process was at least partly associated with CaMKII-dependent phosphorylation.

Measurements of $[Ca^{2+}]_i$ and estimation of SR Ca^{2+} uptake. We have to consider the possible factors that may perturb the present $[Ca^{2+}]_i$ measurement. The first factor was incomplete hydrolysis of indo-1-AM. The myocytes were incubated for 30 min after dye loading at room temperature to gain hydrolyzed fluorescent dye forms. The second factor was compartmentalization of indo-1. In rat ventricular myocytes, the residual fluorescence of indo-1 after treatment of digitonin was reported to be relatively high (40–50% of preexposed level) (33). Therefore, we performed in vivo calibration to get more precise values for $[Ca^{2+}]_i$. The third factor was photobleaching of indo-1 fluorescence. Illumination from the xenon lamp was minimized by neutral density filters, which reduce photobleaching. The diastolic $[Ca^{2+}]_i$ estimated from our method was 75–135 nM, which was nearly identical to that previously reported using fura 2 or indo-1-free acid with patch-clamp technique (6, 15).

The second major problem for $[Ca^{2+}]_i$ measurement in our experiments is the direct effect of pH_i on indo-1 fluorescence (25). We examined in vitro calibration of indo-1 fluorescence both at pH 7.2 and 6.8, and the K_d at pH 6.8 was slightly higher than that at pH 7.2. Because of the factors mentioned above, the in vivo fluorescence ratios at the same $[Ca^{2+}]_i$ somewhat varied (see Fig. 1*C*). To fix both $[Ca^{2+}]_i$ and pH_i in the same cells with the use of ionophores may be possible but incomplete. Thus the obtained fluorescence ratios would vary more extensively. Therefore, we did not make an in vivo calibration at pH_i 6.8 but extrapolated the difference in K_d values obtained at in vitro experiment to the in vivo calibration. Although there is no evidence that the difference in K_d values is identical between in vitro and in vivo situations, our concern was that acidosis increased the apparent K_d for Ca^{2+} binding with little effect on the R_{max} and R_{min}. Because the rapid and stable acidosis was obtained and the in vivo calibration with corrected K_d was applied, we believe that the disturbance of $[Ca^{2+}]_i$ measurement by acidosis was minimized.

Finally, we estimated the SR Ca^{2+} uptake indirectly from the rate of twitch $[Ca^{2+}]_i$ decline. The $[Ca^{2+}]_i$ decline actually expresses Ca^{2+} elimination from the cytoplasm, and Camacho et al. (9) exhibited that there was a linear correlation between time constants of $[Ca^{2+}]_i$ decline and pressure decline in rat perfused hearts. The $[Ca^{2+}]_i$ decline is attributable to the SR Ca^{2+}-ATPase, the Na^+/Ca^{2+} exchanger and the slow systems (sarcolemmal Ca^{2+}-ATPase and mitochondrial Ca^{2+} uniporter). In rat ventricular myocytes, ~90% of Ca^{2+} at normal twitch is eliminated through sequestration into the SR (2). The time constant of twitch $[Ca^{2+}]_i$ decline with single exponential fit can therefore represent the activity of SR Ca^{2+} uptake (2). However, the balance among the Ca^{2+} transport systems might shift during acidosis, and the decrease in cytosolic Ca^{2+} buffering capacity could also affect the Ca^{2+} kinetics (19, 35). These factors would have somewhat blunted the reacceleration of twitch $[Ca^{2+}]_i$ decline. The rate of $[Ca^{2+}]_i$ decline also depends on the peak of CaT (6), and therefore the reacceleration of $[Ca^{2+}]_i$ decline at RP could simply be ascribed to the increase in CaT amplitude. We examined this issue by measuring the decline rate in any given $[Ca^{2+}]_i$ and by plotting the time constants against the peak $[Ca^{2+}]_i$, and concluded that the increase in CaT amplitude cannot explain the reacceleration of twitch $[Ca^{2+}]_i$ decline.

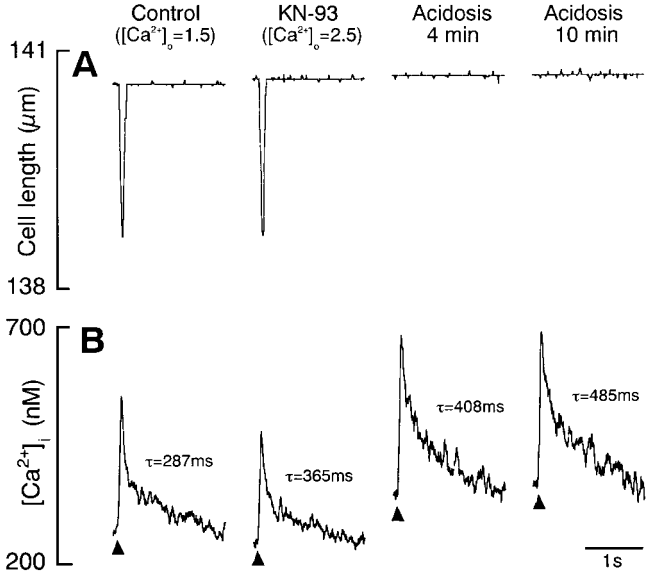

Fig. 8. Effects of 2-[*N*-(2-hydroxyethyl)-*N*-(4-methoxybenzenesulfonyl)]amino-*N*-(4-chlorocinnamyl) methyl benzamine (KN-93) on acidosis-induced changes in twitch cell shortening (*A*) and CaT (*B*). The pretreatment of a myocyte with KN-93 (1 μM) decreased twitch contraction and CaT amplitude, and prolonged the twitch $[Ca^{2+}]_i$ decline. The perfusate $[Ca^{2+}]$ was increased to 2.5 mM to match the steady state contraction and CaT amplitude with values at control (KN-93). The twitch contraction decreased during acidosis and never recovered. The diastolic $[Ca^{2+}]_i$ continued to increase, and the CaT amplitude did not increase significantly. The acidosis further slowed the $[Ca^{2+}]_i$ decline, but reacceleration was never observed.

Table 3. *Effects of respiratory and metabolic acidosis in the presence of KN-93*

	CTL	KN-93	Acidosis	
			4 min (DP)	10 min (RP)
Respiratory acidosis				
Twitch contraction, %	3.8 ± 0.5	3.4 ± 0.5	0.5 ± 0.3†	0.9 ± 0.5†
Diastolic $[Ca^{2+}]_i$, nM	75 ± 20	78 ± 13	148 ± 25†	211 ± 38†‡
Twitch CaT amplitude, nM	198 ± 46	226 ± 36	239 ± 51	240 ± 56
Twitch $[Ca^{2+}]_i$ decline, ms	229 ± 17	323 ± 23*	524 ± 47†	593 ± 55†
Metabolic acidosis				
Twitch contraction, %	2.6 ± 0.3	2.6 ± 0.4	0.0 ± 0.0†	0.4 ± 0.3†
Diastolic $[Ca^{2+}]_i$, nM	102 ± 6	102 ± 7	191 ± 14†	256 ± 17†‡
Twitch CaT amplitude, nM	181 ± 20	194 ± 22	237 ± 30	272 ± 33
Twitch $[Ca^{2+}]_i$ decline, ms	195 ± 5	293 ± 10*	480 ± 28†	507 ± 26†

Values are means ± SE from 11 myocytes in both respiratory (5 rats) and metabolic (4 rats) acidosis. In the presence of 2-[*N*-(2-hydroxyethyl)-*N*-(4-methoxybenzonesulfonyl)] amino-*N*-(4-chlorocinnamyl)-*N*-methyl benzamine (KN-93) (1 μm), perfusate $[Ca^{2+}]$ was increased from 1.5 mM to 2.5 mM to match the SS contraction and CaT amplitude with values at CTL. The contractile recovery over 1% of diastolic length was observed only 3 cells (27%) and 2 cells (18%) in respiratory and metabolic acidosis, respectively ($P < 0.05$ vs. without KN-93 by Fisher's exact test). *$P < 0.05$ vs. CTL, †$P < 0.05$ vs. KN-93, ‡$P < 0.05$ vs. 4 min (DP) by ANOVA, followed by Bonferroni's modified *t*-test.

Inhibition of CaMKII by KN-93. In this study, we used KN-93, an isoquinoline sulfonamide derivative, at the concentration of 1 μM to inhibit CaMKII. KN-93 elicits a potent inhibition on CaMKII by competing with calmodulin [inhibitory constant (K_i); 0.37 μM]. The K_i values of KN-93 for other protein kinases, such as PKA, protein kinase C, and myosin light-chain kinase, are all >30 μM (39). Therefore, the dosage we used seemed to be specific to CaMKII, but the inhibition against the CaMKII-dependent reactivation of SR Ca^{2+} uptake (and/or SR Ca^{2+} release) might be incomplete. Actually, some myocytes showed contractile recovery during prolonged acidosis. In these cells, the CaT amplitude tended to increase from DP to RP (data not shown), although the prolonged twitch $[Ca^{2+}]_i$ decline never reaccelerated.

Contractile recovery during prolonged acidosis. During prolonged acidosis, the initially decreased twitch contraction slowly recovered, and this recovery was accompanied by a continuous increase in CaT amplitude. The diastolic cell lengths did not alter presumably because of reduced Ca^{2+} responsiveness of contractile proteins (12, 34). Hulme and Orchard (19) suggested that although acidosis inhibits both SR Ca^{2+} uptake and CICR from the SR, these effects are compensated by an increase in SR Ca^{2+} content secondary to a rise in $[Ca^{2+}]_i$. Indeed, we documented that the SR Ca^{2+} content (evaluated with caffeine-induced CaT) continued to increase during acidosis, and the inhibition of SR function completely abolished the contractile recovery. However, there was a cell-to-cell heterogeneity in the contractile recovery both in respiratory and metabolic acidosis. In Rec, the CaT amplitude increased further and the twitch $[Ca^{2+}]_i$ decline reaccelerated from DP to RP, whereas in NRec these changes did not occur. In contrast, the increase in diastolic $[Ca^{2+}]_i$ was more extensive in NRec. Thus the increase in $[Ca^{2+}]_i$ is not the sole mechanism for the contractile recovery; however, reactivation of SR Ca^{2+} uptake seems to be crucial, although we could not compare the SR Ca^{2+} contents between Rec and NRec.

Reactivation of SR Ca^{2+} uptake during prolonged acidosis. The SR Ca^{2+} uptake is activated through phosphorylation of PLB and can also be stimulated by direct phosphorylation of SR Ca^{2+}-ATPase. The PLB and SR Ca^{2+}-ATPase are mainly phosphorylated by PKA (28, 38), CaMKII (4, 27, 41, 43), and are dephosphorylated by protein phosphatase-1 (PP1) (29, 32). Because acidosis increased $[Ca^{2+}]_i$, and the reacceleration of twitch $[Ca^{2+}]_i$ decline was prevented under phosphorylated state, the CaMKII-dependent phosphorylation was thought to be primary for the reactivation of SR Ca^{2+} uptake. The importance of endogenous CaMKII for normal excitation-contraction coupling has been reported in intact mouse and ferret myocytes (26, 27). Actually, KN-93 prolonged the twitch $[Ca^{2+}]_i$ decline at control perfusion and abolished its reacceleration at prolonged acidosis (Fig. 7 and Table 3).

PLB phosphorylation has been studied extensively in vitro, but little is known about the role in intact myocytes. Previous in vitro studies (28, 31, 41, 42) have indicated that cAMP-dependent (Ser^{16}) and CaMKII-dependent (Thr^{17}) phosphorylation of PLB could occur independently, but interventions that increase $[Ca^{2+}]_i$ by cAMP-independent mechanism failed to alter PLB phosphorylation. Furthermore, Mundiña-Weilenmann et al. (30) exhibited that acidosis had no effect on the phosphorylation of PLB in the absence of isoproterenol, suggesting that CaMKII-dependent phosphorylation of PLB can only occur when cAMP levels increased within the cell.

However, the involvement of PKA-dependent phosphorylation of PLB is unlikely because acidosis reportedly does not alter the cAMP content of the heart (30), and also reduces the phosphorylation of Ser^{16} (18). On the other hand, recent studies (4, 26) in intact cardiomyocytes have shown evidence that CaMKII does activate SR Ca^{2+} uptake both in the presence and absence (knockout model) of PLB. Furthermore, Hulme et al. (18) demonstrated that acidosis increased phosphorylation of Thr^{17}, which was abolished by buffering

cytoplasmic Ca^{2+}. In addition, Mundiña-Weilenmann et al. (30) reported that acidosis inhibits PP1 activity. The dynamic modulation of excitation-contraction coupling by protein phosphatases has been demonstrated (10, 32). In the experiments regarding the role of phosphorylation for reactivation of SR Ca^{2+} uptake (Fig. 5 and Table 2), we used cantharidin to exclude the possible inhibition of PP1 by acidosis. Indeed, the modulation of twitch contraction and CaT by cantharidin was small under control condition, and was lacking in the maximally phosphorylated state by isoproterenol. However, if the phosphorylation of SR proteins by CaMKII was submaximal, the acidosis-induced inhibition of PP1 could affect it. We therefore consider that during prolonged acidosis, the activation of CaMKII by increased $[Ca^{2+}]_i$, coupled with suppressed PP1 activity, phosphorylated PLB and SR Ca^{2+}-ATPase, and reactivated the SR Ca^{2+} uptake. The cell-to-cell heterogeneity in the contractile recovery could be explained by the difference in activation of CaMKII and/or inhibition of PP1.

CaMKII also phosphorylates the L-type Ca^{2+} channels and the SR Ca^{2+} release channels, and facilitates the Ca^{2+} current and the CICR from the SR (14, 27, 45). The CaMKII-induced activation of these Ca^{2+} fluxes could actually contribute to the contractile recovery during prolonged acidosis. More controlled studies are necessary to clarify this issue, because SR Ca^{2+} load can strongly affect the CICR (3), and Ca^{2+} released from the SR can also alter gating of the sarcolemmal Ca^{2+} channels (5).

Physiological implications. Control of pH_i is important in all tissues for optimal functioning of metabolic enzymes, contractile elements, protein synthesis, and ion conductivity (21). Myocardial acidosis caused by ischemia, renal, or respiratory failure has generally been considered detrimental. Our finding that the CaMKII-induced reactivation of SR Ca^{2+} uptake increased the CaT amplitude and limited the contractile dysfunction proposes a compensatory reaction of myocytes against the decreased Ca^{2+} responsiveness of contractile protein. The prevention of extensive increase in diastolic $[Ca^{2+}]_i$ may also provide a protective mechanism against cellular Ca^{2+} overload.

However, the increase in $[Ca^{2+}]_i$ and reactivation of SR Ca^{2+} uptake during prolonged acidosis could cause the pH paradox by activating Ca^{2+}-dependent degradative enzymes and by inducing spontaneous Ca^{2+} release from the SR, respectively. Actually, the rapid return to physiological pH_i resulted in hyper and spontaneous contractions, and in some cells hypercontracture. Previous studies have shown that reperfusion with acidic solution or with inhibitors of Na^+/H^+ exchange is protective for ischemic myocardium against reperfusion cell injury. These interventions prevent activation of degradative enzymes and subsequent destructive processes, and Ca^{2+} overload via Na^+/Ca^{2+} exchange (see Ref. 22 for a review).

In conclusion, although acidosis initially inhibits both SR Ca^{2+} uptake and sarcolemmal Ca^{2+} extrusion, the SR Ca^{2+} uptake recovers during prolonged acidosis, which increases CaT amplitude and reaccelerates twitch $[Ca^{2+}]_i$ decline. This recovery of SR Ca^{2+} cycling can compensate for the decreased Ca^{2+} responsiveness of contractile proteins, but may also cause Ca^{2+} overload after returning to physiological pH_i. The involvement of CaMKII is suggested, but other possible mechanisms and their physiological implications should be investigated further.

The authors thank Dr. Donald M. Bers and Dr. Hideki Katoh for the critical reading of this manuscript.

This study was supported by the Japan Heart Foundation and Pfizer Pharmaceuticals Grant for Research on Coronary Artery Disease, and by Ministry of Education, Culture, and Science of Japan Grant-in-Aid 11670670 (to H. Satoh).

REFERENCES

1. **Balnave CD and Vaughan-Jones RD.** Effect of intracellular pH on spontaneous Ca^{2+} sparks in rat ventricular myocytes. *J Physiol* 528: 25–37, 2000.
2. **Bassani JWM, Bassani RA, and Bers DM.** Relaxation in rabbit and rat cardiac cells: species-dependent differences in cellular mechanisms. *J Physiol* 476: 279–293, 1994.
3. **Bassani JWM, Yuan W, and Bers DM.** Fractional SR Ca release is regulated by trigger Ca and SR Ca content in cardiac myocytes. *Am J Physiol Cell Physiol* 268: C1313–C1329, 1995.
4. **Bassani RA, Mattiazzi A, and Bers DM.** CaMKII is responsible for activity-dependent acceleration of relaxation in rat ventricular myocytes. *Am J Physiol Heart Circ Physiol* 268: H703–H712, 1995.
5. **Bers DM.** *Excitation-Contraction Coupling and Cardiac Contractile Force*. Norwell, MA: Kluwer, 1991.
6. **Bers DM and Berlin JR.** Kinetics of $[Ca^{2+}]_i$ decline in cardiac myocytes depend on peak $[Ca^{2+}]_i$. *Am J Physiol Cell Physiol* 268: C271–C277, 1995.
7. **Boknik P, Khorchidi S, Bodor GS, Huke S, Knapp J, Linck B, Lüss H, Müller FU, Schmitz W, and Nuemann J.** Role of protein phosphatases in regulation of cardiac inotropy and relaxation. *Am J Physiol Heart Circ Physiol* 280: H786–H794, 2001.
8. **Bond JM, Chacon E, Herman B, and Lemasters J.** Intracellular pH and Ca^{2+} homeostasis in the pH paradox of reperfusion injury to neonatal rat cardiac myocytes. *Am J Physiol Cell Physiol* 265: C129–C137, 1993.
9. **Camacho SA, Brandes R, Figueredo VM, and Weiner MW.** Ca^{2+} transient decline and myocardial relaxation are slowed during low flow ischemia in rat hearts. *J Clin Invest* 93: 951–957, 1994.
10. **DuBell WH, Lederer WJ, and Rogers TB.** Dynamic modulation of excitation-contraction coupling by protein phosphatases in rat ventricular myocytes. *J Physiol* 493: 793–800, 1996.
11. **Evans AM and Cannell MB.** The role of L-type Ca^{2+} current and Na^+ current-stimulated Na^+-Ca^{2+} exchange in triggering SR calcium release in guinea-pig cardiac ventricular myocytes. *Cardiovasc Res* 35: 284–302, 1997.
12. **Fabiato A and Fabiato F.** Effects of pH on the myofilaments and sarcoplasmic reticulum of skinned cells from cardiac and skeletal muscles. *J Physiol* 276: 233–255, 1978.
13. **Grynkiewicz G, Poenie M, and Tsien RY.** A new generation of Ca^{2+} indicators with greatly improved fluorescence properties. *J Biol Chem* 260: 3440–3450, 1985.
14. **Hain J, Onoue H, Mayrleitner M, Fleischer S, and Schindler H.** Phosphorylation modulates the function of the calcium release channel of sarcoplasmic reticulum from cardiac muscle. *J Biol Chem* 270: 2074–2081, 1995.
15. **Harrison SM, Frampton JE, McCall E, Boyett MR, and Orchard CH.** Contraction and intracellular Ca^{2+}, Na^+, and H^+ during acidosis in rat ventricular myocytes. *Am J Physiol Cell Physiol* 262: C348–C357, 1992.
16. **Hayashi H, Miyata H, Noda N, Kobayashi A, Hirano M, Kawai T, and Yamazaki N.** Intracellular Ca^{2+} concentration

and pH_i during metabolic inhibition. *Am J Physiol Cell Physiol* 262: C628–C634, 1992.
17. **Hess P, Lansman JB, and Tsien RW.** Different modes of Ca channel gating behaviour favoured by dihydropyridine Ca agonists and antagonists. *Nature* 311: 538–544, 1984.
18. **Hulme JT, Colyer J, and Orchard CH.** Acidosis alters the phosphorylation of Ser^{16} and Thr^{17} of phospholamban in rat cardiac muscle. *Pflügers Arch* 434: 475–483, 1997.
19. **Hulme JT and Orchard CH.** Effect of acidosis on Ca^{2+} uptake and release by sarcoplasmic reticulum of intact rat ventricular myocytes. *Am J Physiol Heart Circ Physiol* 275: H977–H987, 1998.
20. **Irisawa H and Sato R.** Intra- and extracellular actions of proton on the calcium current of isolated guinea-pig ventricular cells. *Circ Res* 59: 348–355, 1986.
21. **Karmazyn M and Moffat MP.** Role of Na^+/H^+ exchange in cardiac physiology and pathophysiology: mediation of myocardial reperfusion injury by the pH paradox. *Cardiovasc Res* 27: 915–924, 1993.
22. **Karmazyn M, Gan XT, Humphreys RA, Yoshida H, and Kusumoto K.** The myocardial Na^+-H^+ exchange structure, regulation, and its role in heart disease. *Circ Res* 85: 777–786, 1999.
23. **Katoh H, Terada H, Iimuro M, Sugiyama S, Qing K, Satoh H, and Hayashi H.** Heterogeneity and underlying mechanism for inotropic action of endothelin-1 in rat ventricular myocytes. *Br J Pharmacol* 123: 1343–1350, 1998.
24. **Kohmoto O, Spitzer KW, Movsesian MA, and Barry W.** Effects of intracellular acidosis on $[Ca^{2+}]_i$ transients, transsarcolemmal Ca^{2+} fluxes, and contraction in ventricular myocytes. *Circ Res* 66: 622–632, 1990.
25. **Lattanzio FA Jr.** The effects of pH and temperature on the fluorescent calcium indicators as determined with chelex-100 and EDTA buffer systems. *Biochem Biophys Res Commun* 171: 102–108, 1990.
26. **Li L, Chu G, Kranias EG, and Bers DM.** Cardiac myocyte calcium transport in phospholamban knockout mouse: relaxation and endogeneous CaMKII effects. *Am J Physiol Heart Circ Physiol* 274: H1335–H1347, 1998.
27. **Li L, Satoh H, Ginsburg KS, and Bers DM.** The effect of Ca^{2+}-calmodulin dependent protein kinase II on cardiac excitation-contraction coupling in ferret ventricular myocytes. *J Physiol* 501: 17–32, 1997.
28. **Lindemann JP, Jones LR, Hathway DR, Henry BG, and Watanabe AM.** β-adrenergic stimulation of phospholamban phosphorylation and Ca^{2+}-ATPase activity in guinea pig ventricles. *J Biol Chem* 258: 464–471, 1983.
29. **MacDougall LK, Jones LR, and Cohen P.** Identification of the major protein phosphatases in mammalian cardiac muscle which dephosphorylates phospholamban. *Eur J Biochem* 196: 725–734, 1991.
30. **Mundiña-Weilenmann C, Vittone L, Cingolani HE, and Orchard CH.** Effects of acidosis on phosphorylation of phospholamban and troponin I and in rat cardiac muscle. *Am J Physiol Cell Physiol* 270: C107–C114, 1996.
31. **Napolitano R, Vittone L, Mundina C, Chiappe de Cingolani G, and Mattiazzi A.** Phosphorylation of phospholamban in the intact heart. A study on the physiological role of the Ca^{2+}-calmodulin-dependent protein kinase system. *J Mol Cell Cardiol* 24: 387–396, 1992.
32. **Neumann J, Boknik P, S, Herzig Schmitz W, Scholz H, Gupta RC, and Watanabe AM.** Evidence for physiological functions of protein phosphatases in the heart: evaluation with ocadaic acid. *Am J Physiol Heart Circ Physiol* 265: H257–H266, 1993.
33. **Noda N, Hayashi H, Satoh H, Terada H, Hirano M, Kobayashi A, and Yamazaki N.** Ca^{2+} transients and cell shortening in diabetic rat ventricular myocytes. *Jpn Circ J* 57: 449–457, 1993.
34. **Orchard CH, Hamilton DL, Astles P, McCall E, and Jewell BR.** The effect of acidosis on the relationship betwen calcium and force in isolated ferret cardiac muscle. *J Physiol* 436: 559–578, 1991.
35. **Orchard CH and Kentish JC.** Effects of changes of pH on the contractile function of cardiac muscle. *Am J Physiol Cell Physiol* 258: C967–C981, 1990.
36. **Satoh H, Hayashi H, Katoh H, Terada H, and Kobayashi A.** Na^+/H^+ and Na^+/Ca^{2+} exchange in regulation of $[Na^+]_i$ and $[Ca^{2+}]_i$ during metabolic inhibition. *Am J Physiol Heart Circ Physiol* 268: H1239–H1248, 1995.
37. **Schulman H, Hanson PI, and Meyer T.** Decoding calcium signals by multifunctional CaM kinase. *Cell Calcium* 13: 401–411, 1992.
38. **Simmerman HK, Collins JH, Theibert JL, Wegener AD, and Jones LR.** Sequence analysis of phospholamban. Identification of phosphorylation sites and two major structural domains. *J Biol Chem* 261: 13333–13341, 1986.
39. **Sumi M, Kiuchi K, Ishikawa T, Ishii A, Hagiwara M, Nagatsu T, and Hidaka H.** The newly synthesized selective Ca^{2+}/calmodulin-dependent protein kinase II inhibitor KN-93 reduces dopamine contents in PC12h cells. *Biochem Biophys Res Commun* 181: 968–975, 1991.
40. **Tada M, Yamada M, Kodama M, Inui M, and Ohmori F.** Calcium transport by cardiac sarcoplasmic reticulum and phosphorylation of phospholamban. *Mol Cell Biochem* 46: 73–95, 1982.
41. **Vittone L, Cecilia M, Chiappe de Cingoloni G, and Mattiazi A.** cAMP and calcium-dependent mechanisms of phospholamban phosphorylation in intact hearts. *Am J Physiol Heart Circ Physiol* 258: H318–H325, 1990.
42. **Vittone L, Mundiña-Weilenmann C, Said M, and Mattiazzi A.** Mechanisms involved in the acidosis enhancement of the isoproterenol-induced phosphorylation of phospholamban in the intact heart. *J Biol Chem* 273: 9804–9811, 1998.
43. **Xu A, Hawkins C, and Narayanan N.** Phosphorylation and activation of the Ca^{2+}-pumping ATPase of cardiac sarcoplasmic reticulum by Ca^{2+}/calmodulin-dependent protein kinase. *J Biol Chem* 268: 8394–8397, 1993.
44. **Xu L, Mann G, and Meissner G.** Regulation of cardiac Ca^{2+} release channel (ryanodine receptor) by Ca^{2+}, H^+, Mg^{2+}, and adenine nucleotides under normal and simulated ischemic conditions. *Circ Res* 79: 1100–1109, 1996.
45. **Yuan W and Bers DM.** Ca-dependent facilitation of cardiac Ca current is due to Ca-calmodulin-dependent protein kinase. *Am J Physiol Heart Circ Physiol* 267: H982–H993, 1994.